Tuning Magnetic Order and Spin–Exciton Interactions in $MnPSe_3$ via Cu Substitution

Mohamed Nawwar,[a] Alexander Blackston,[a] Sogol Lotfi, [a] Xiling Deng,[a] Alexander Reifsnyder,[a] David McComb,[a] Wolfgang Windl,[a,b] Vicky Doan-Nguyen Trigg,[a] and Roberto C. Myers[a,b,c*]

[a] *Department of Materials Science and Engineering, The Ohio State University, Columbus OH 43210 USA*

[b] *Department of Physics, The Ohio State University, Columbus OH 43210 USA*

[c] *Department of Electrical and Computer Engineering, The Ohio State University, Columbus OH 43210 USA*

∗ Corresponding author

I. ADDITIONAL STRUCTURAL CHARACTERIZATION DATA

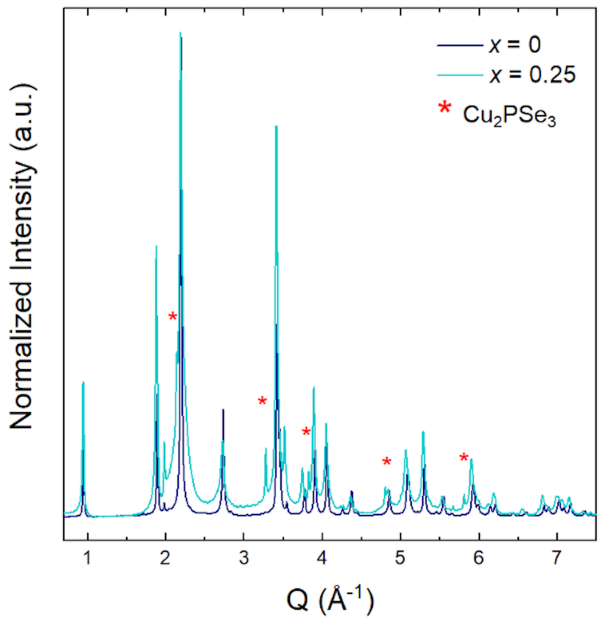

FIG. 1. XRD pattern for $x = 0.25$ sample. Red asterisk indicates the formation of Cu_2PSe_3 impurities

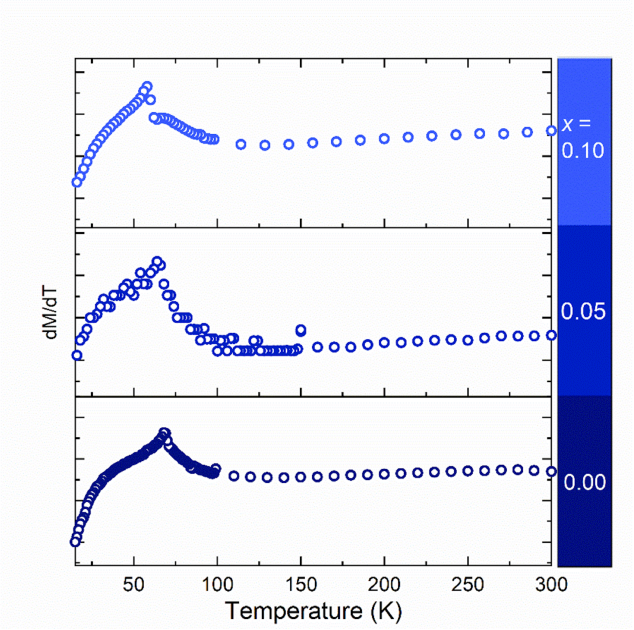

FIG. 2. Derivative of magnetic moment as a function of temperature. Néel temperature is determined by finding the maximum point in the data

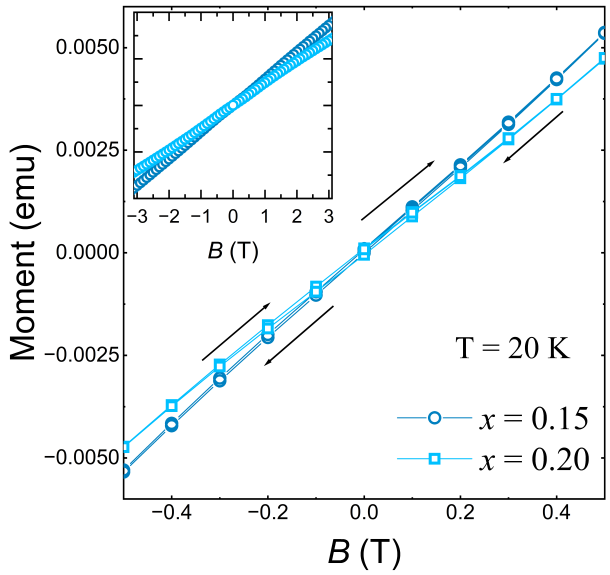

FIG. 3. Magnetic hysteresis curve for x = 0.15 and 0.2 samples. No hysteresis was observed indicating absence of any ferromagnetic moment in the sample

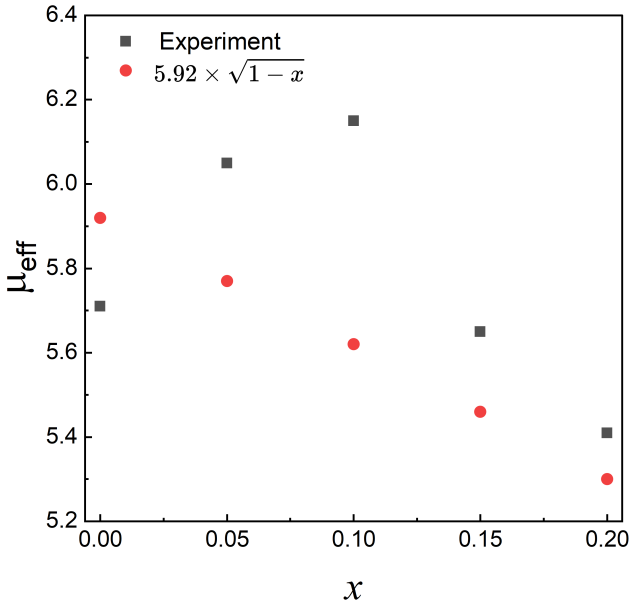

FIG. 4. Effective magnetic moment as a function of X as determined from Curie-Weiss. Red points are the calculated moment assuming Mn^{2+} ions with x vacancies.

TABLE I. Lattice parameters for $Mn_{1-x}Cu_{2x}PSe_3$

x	a Å	c Å
0	6.3856(3)	20.051(1)
0.05	6.3862(6)	20.088(2)
0.1	6.3960(3)	20.141(2)
0.15	6.3917(7)	20.153(2)
0.2	6.4039(5)	20.219(2)

II. FITTING AND ANALYSIS OF INTERFERENCE FRINGES

As is typical with thin film materials, the absorption data collected in the weak absorption region below the band gap contained interference effects that gave rise to a characteristic set of fringes. The PRISA software package developed by S.Jena et al that employs the well known Swanepoel envelope method for retrieving the optical absorption spectrum from weak absorption regions with interference fringes was used extract the weak absorption region spectrum and determine the thickness of the flake (sup. fig. 3).[1] This method works by fitting the maxima and minima of the interference fringes with upper and lower envelopes that pass through them tangentially. The resulting upper (T_M) and lower (T_M) envelope curves can then be used to approximate the index of refraction (n) of the material within the spectral region where interference fringing occurs using the following set of equations,

$$n = \sqrt{N + \sqrt{N^2 - {n_s}^2}} \tag{1}$$

where,

$$N = 2n_s \frac{T_M - T_m}{T_M T_m} + \frac{{n_s}^2 + 1}{2} \tag{2}$$

given that n_S is the known wavelength dependent index of refraction of the substrate material "in our study- glass."

Once n has been calculated, it is also possible approximate the sample thickness (d) by selecting two adjacent interference fringe maxima or minima and recording their wavelengths λ_1 and λ_2 where $\lambda_1 > \lambda_2$. Taking the index of refraction at these two extrema, n(λ_1) and n(λ_2), d can be calculated,

$$d = \frac{\lambda_1 \lambda_2}{2[\lambda_1 n(\lambda_1) - \lambda_2 n(\lambda_2)]} \tag{3}$$

Similarly the extinction coefficient (k) can be approximated once n and d are known via the following equations,

$$k = -\frac{\lambda}{4\pi d} ln(x) \tag{4}$$

where,

$$x = \frac{F - \sqrt{F^2 - [(n^2 - 1)^3 (n^2 - {n_s}^4)]}}{(n-1)^3 (n - {n_s}^2)} \tag{5}$$

and

$$F = 4n^2 n_s \frac{T_M + T_m}{T_M T_m} \tag{6}$$

Finally, the wavelength dependent absorption coefficient can be calculated from k,

$$\alpha(\lambda) = \frac{4\pi k}{\lambda} \tag{7}$$

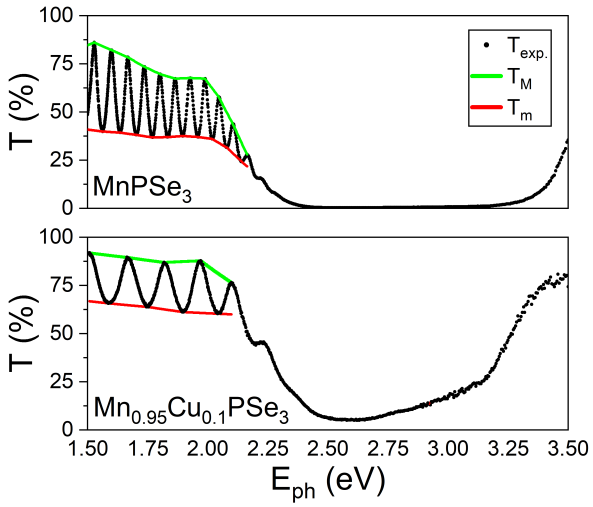

FIG. 5. Experimentally measured transmittance (T_{exp} of the $MnPSe_3$ and $Mn_{0.95}Cu_{0.1}PSe_3$ samples and the constructred upper and lower envelope functions, T_M and T_m, fit using PRISA software.

Using the extracted absorption spectra, the optical band gap (E_{g-opt}) of both samples was approximated via the Tauc method. [2] The band edge absorption data is fit to obtain E_{g-opt} according to the equation,

$$(\alpha \cdot E_{ph})^{1/\gamma} = B(E_{ph} - E_{g-opt}) \tag{8}$$

where B is a constant and γ has been set to $\frac{1}{2}$ due to the direct nature of $MnPSe_3$'s band gap (sup. fig. 4).

III. ELECTRONIC STRUCTURE CALCULATIONS.

First-principles calculations of the $Mn_{24-n}Cu_{2n}P_{24}Se_{72}$ ($n = 0, \ldots, 3$) alloys were carried out within density functional theory (DFT) using the VASP code as shown in figure 7.[3] For each composition, representative disordered configurations were generated as special quasi-random structures (SQS) using the MCSQS module of the ATAT package,[4, 5] ensuring near-random short-

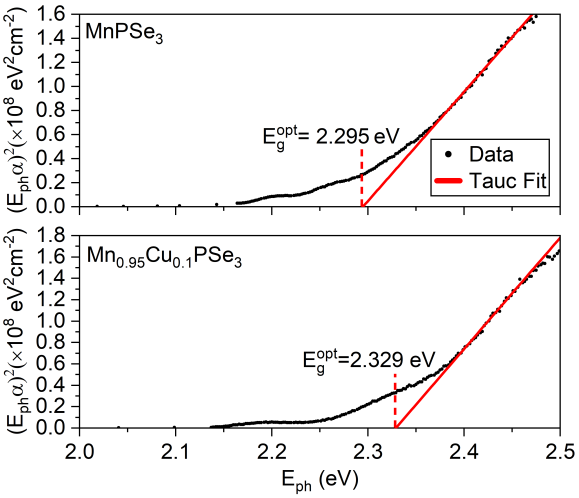

FIG. 6. Tauc plots of absorption edge used to estimate the optical band gap ($E_g{}^{opt}$) of the flakes.

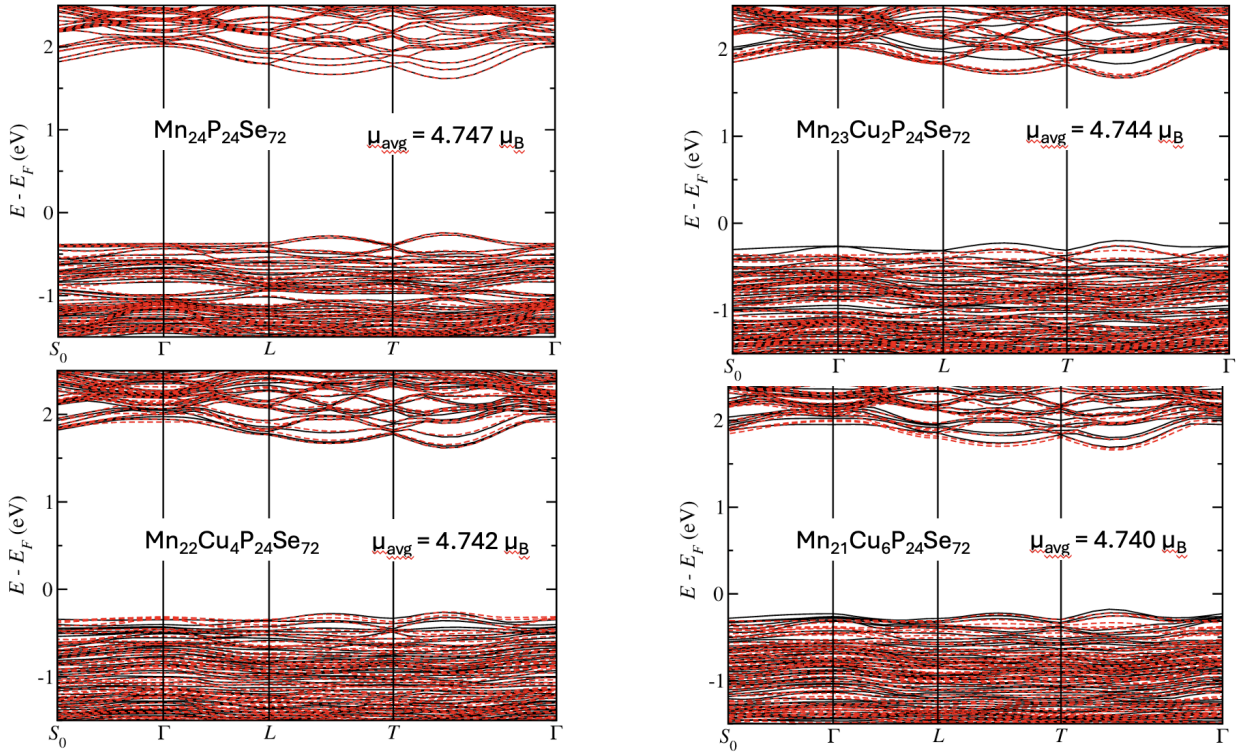

FIG. 7. DFT calculations of the band structure of Cu-substituted $MnPSe_3$ along with their corresponding magnetic moment. The moment here represents each Mn ion and not the overall effective moment.

range order of Mn and Cu sites.

All structures were relaxed until atomic forces were below 0.02 eV Å^{-1} and total energy changes below 10^{-5} eV. A Γ-centered $6 \times 6 \times 1$ Monkhorst–Pack k-point mesh was used for Brillouin-zone sampling, and a plane-wave energy cutoff of 500 eV ensured well-converged total energies and band structures.

Spin polarization was included in all calculations. For each SQS configuration, several initial magnetic moment assignments on the Mn and Cu atoms were tested, and the lowest-energy magnetic configuration was adopted for subsequent electronic-structure analysis. Band structures were then computed for the fully relaxed geometries using the same convergence parameters.

Figure 7 shows minimal change in the electronic structure on substituting more copper. Additionally, the magnetic moment of each Mn ion shows no change. This is consistent with our analysis that the charge of Mn ion does not change while the main parameters that changes are the magnetic exchange interactions. DFT-calculated convex hull for substituted structures confirms that substituting a single Cu atom for Mn is energetically unfavorable, as indicated by the positive formation energies (Figure 8). In contrast, substitution with 2 cu atoms yields negative formation energies across the studied range ($x \leq 2.5$).

A. Choice of the Hubbard U parameter.

On-site Coulomb interactions were treated using the rotationally invariant DFT+U formalism of Dudarev *et al.*,[6] where $U_{\text{eff}} = U - J$. A value of $U_{\text{eff}} = 4$ eV was initially applied to the Mn $3d$ states, consistent with previous

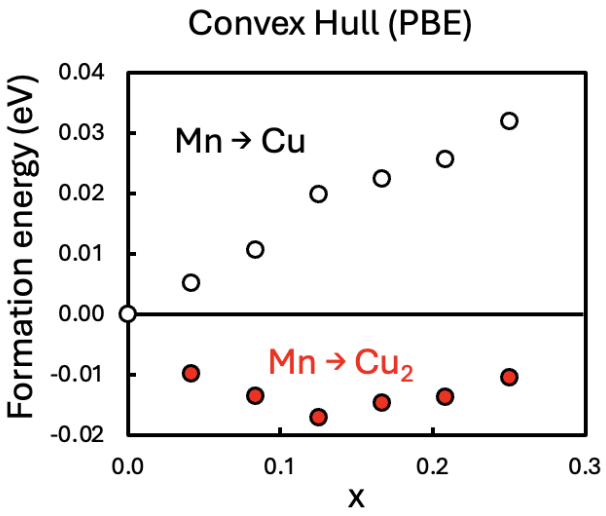

FIG. 8. DFT calculations of the formation energies for Mn with one Cu atom (white circles) and 2 Cu atoms (red circles). The negative formation energies for the two-atom substitution indicate a thermodynamically favorable system, whereas the single-atom substitution remains energetically unfavorable.

studies of Mn-based chalcogenides, to correct the over-delocalization of Mn d electrons in standard GGA. To assess the sensitivity of the electronic structure to this parameter, test calculations were performed for $U_{\text{eff}} = 0$–5 eV on representative SQS cells ($n = 0$ and $n = 4$). The chosen value of 4 eV yields stable high-spin Mn moments ($\sim 4-5\ \mu_B$), physically reasonable Mn–Se hybridization near the valence-band edge, and does not alter the relative stability of competing magnetic configurations. Cu $3d$ orbitals were not corrected, as their fully filled $3d^{10}$ shells lie well below the Fermi level and exhibit negligible self-interaction error. Once selected, the same U_{eff} value was used consistently across all compositions to ensure comparable energetics.

IV. BIBLIOGRAPHY

[1] S. Jena, R. Tokas, S. Thakur and D. Udupa, PRISA: a user-friendly software for determining refractive index, extinction co-efficient, dispersion energy, band gap, and thickness of semiconductor and dielectric thin films, *Nano Express*, 2021, **2**, 010008.

[2] P. Makuła, M. Pacia and W. Macyk, *How to correctly determine the band gap energy of modified semiconductor photocatalysts based on UV–Vis spectra*, 2018.

[3] G. Kresse and J. Furthmüller, Efficient iterative schemes for ab initio total-energy calculations using a plane-wave basis set, *Physical review B*, 1996, **54**, 11169.

[4] A. Zunger, S.-H. Wei, L. G. Ferreira and J. E. Bernard, Special quasirandom structures, *Physical review letters*, 1990, **65**, 353.

[5] A. van de Walle and G. Ceder, Automating first-principles phase diagram calculations, *Journal of Phase Equilibria*, 2002, **23**, 348.

[6] S. L. Dudarev, G. A. Botton, S. Y. Savrasov, C. Humphreys and A. P. Sutton, Electron-energy-loss spectra and the structural stability of nickel oxide: An LSDA+ U study, *Physical Review B*, 1998, **57**, 1505.